

A Novel Robot Gripper with Scott Linkage for Scooping and Self-Adaptive Grasp in Environmental Constraints *

Shijie Qu and Wenzeng Zhang, Member, IEEE

Abstract—This paper introduces Gamma-X, a forward-driven, two-fingered gripper designed to address the challenge of grasping thin, flat objects resting on planar surfaces. Each finger integrates a Scott-Russell straight-line mechanism, a parallelogram linkage, and dual-motor actuation, enabling three key innovations. The Scott-Russell mechanism imparts a left-diagonal trajectory to the fingertip, enhancing passive compliance during environmental interaction. This design mitigates rigid impact shocks and adapts to irregular surfaces by absorbing contact forces. The parallelogram linkage, augmented with stopper blocks and elastic elements, introduces a unidirectional flipping capability for the fingertip segment. This feature can be triggered passively or actively, facilitating a transition from precision pinching to scooping postures. Gamma-X executes grasping tasks primarily through linear actuation of its primary motor, supporting multiple grasping modes: precision pinching, scooping, and adaptive enveloping. Experimental results confirm its ability to reliably manipulate thin objects on flat surfaces such as desktops. The gripper's design minimizes reliance on complex control algorithms while offering advantages of compactness, cost-efficiency, and operational simplicity. This hardware solution provides a robust alternative for grasping flat-lying objects in both domestic and industrial applications.

I. INTRODUCTION

Grasping thin, flat objects lying in constrained environments has long been a challenge. Unlike many robotic grasping demonstrations where objects are ideally suspended in mid-air, real-world objects often lie tightly conforming to supporting surfaces (such as desktops, conveyor belts, etc.). For mainstream robotic hands composed of rigid components, achieving operations that can effectively resist contact impacts while adjusting posture to complete grasps under such constraints presents significant difficulties.

In recent years, numerous teams have dedicated efforts to the challenge of achieving stable grasping and scooping in unstructured scenarios: Some teams focus on robotic arm control and algorithm design. For instance, Wei Jia et al. implemented grasping in constrained environments for a humanoid robot arm using three complementary trajectory strategies [1]. Yuto Kageyama et al. enabled traditional robotic arms to perform scooping actions after gripping a

spoon through algorithmic design [2]. These studies achieve scooping through the development of robotic arm control algorithms. On the other hand, other teams have explored whether the robotic hand itself can achieve scooping. For example, Prof. Dalle's team designed serrated structures on the fingertips and used one finger to block cards, allowing objects to flip on the fingertips [3]. Qi Zhang's team conducted research with a similar principle, enabling scooping for sheet objects through coordinated action of two fingers [4]. Golline kept the robotic arm angle fixed and designed fingertips to insert beneath objects to lift them [5]. Vincent Babin built upon this model with finger designs allowing active bending of the fingertip to adapt to desktop environments, thereby completing object grasping [6]. Hyeonje based on tilting the robotic arm, redesigned mechanical fingertips and accelerated arm movement to achieve scooping by inserting fingertips beneath objects [7]. Tierui controlled robotic arm angles and employed a retractable finger mechanism to insert fingertips beneath objects for scooping [8][9]. Leonardo utilized two spoon-shaped jaws combined with pneumatic actuation for food transfer [10]. Tianyi Ko enabled in-hand manipulation via friction by installing conveying devices on the fingertips [11].

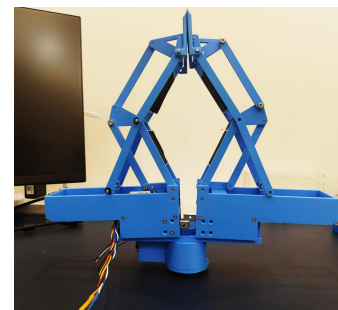


Figure 1. The Gamma-X gripper

Moreover, many research teams have concentrated on suction cup gripper designs. In the 1st Amazon Picking Challenge, numerous teams utilized suction cup grippers or added thin sheets with an angle of attack to the ends of parallel grippers to mimic fingertips for grasping [12]. Some teams have also explored combining electrostatic adhesion with suction cups in their gripper designs. However, suction cups and electrostatic adhesion still struggle to grip objects with complex surfaces and often require assistance from other fingers. that integrated suction cups with adhesive fluid, enabling the grasping of thin and lightweight objects through suction [13]. As can be seen from the above studies, although many solutions have been developed for grasping thin and lightweight objects, rigid collisions pose a significant challenge for mechanical grippers, which often rely on precise control.

* Research supported by Enhanced Student Research Training (E-SRT) and Foundation of Open Research for Innovation Challenges (ORIC), X-Institute.

Shijie Qu is with School of Big Date and Internet, Shenzhen Technology University, Shenzhen, China and Laboratory of Robotics, X-Institute, Shenzhen, China.

Wenzeng Zhang is with Laboratory of Robotics, X-Institute, Shenzhen, China and Dept. of Mechanical Engineering, Tsinghua University, Beijing, China (Corresponding author, email: zhangwenzeng@x-institute.edu.cn).

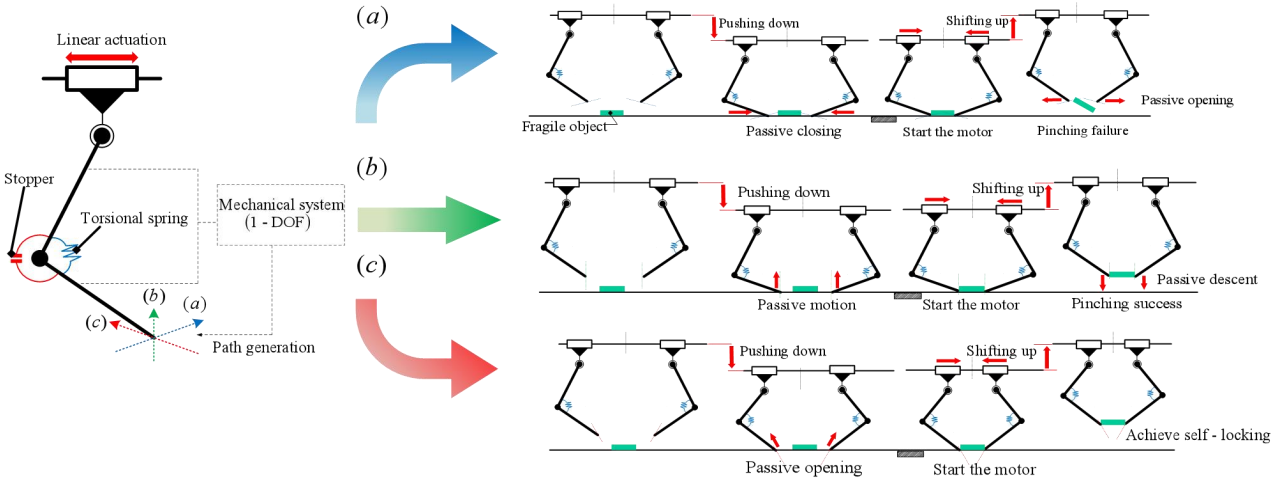


Figure 2. Possible movements of two - phalanx fingers based on fingertip paths. (a) Right diagonal path (b) Vertical path (c) Left diagonal path.

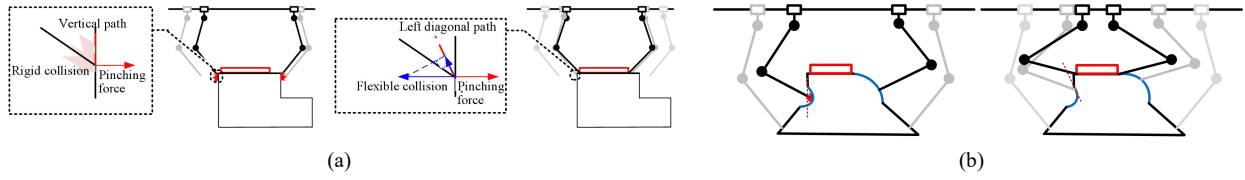


Figure 3. Fingers with a left diagonal path can adapt to more complex environments compared to those with a vertical path.

Grasping in constrained environments is, to this day, an ongoing research topic. Objects can rarely be grasped from arbitrary directions, hence the need to study the options available to grasp them" [14] To address the challenges in thin and lightweight object grasping, it is essential to develop a mechanical gripper that is insensitive to rigid collisions, low-cost, simple to control, and provides stable and powerful grasping capabilities.

The OMEGA hand by Keehoon inspired research into compliant fingertip mechanisms for environmental interaction [15], offering new insights for rigid robotic hands to counteract environmental impacts. However, the OMEGA hand exhibits notable shortcomings: its evaluation of fingertip trajectory effectiveness lacks empirical comparative analysis and appears arbitrary; the Hart's linkage mechanism employed for achieving straight-line end trajectories involves overly complex parameter design and excessive linkages, increasing manufacturing costs; moreover, it fails to achieve scooping in scenarios lacking direct environmental interaction. Building upon this research, our device explores and innovates with the following key advancements:

1) A second motor is added to each individual finger to actuate the base link of the parallelogram linkage, endowing the fingertip segment with active flipping capability.

2) The compliant trajectory of the fingertip is inwardly inclined, providing pressure when lifting objects at the fingertip, thereby enhancing grasp stability and efficiency.

3) The Scott-Russell mechanism replaces the Hart's linkage; determining its end trajectory does not rely on complex mathematical principles, and as a three-bar linkage, it has low manufacturing costs.

We name this gripper Gamma-X. In Section 2 of this paper, the rationale for selecting the inwardly inclined trajectory for the fingertip segment is analyzed. Section 3 explains the mathematical principles behind determining the end trajectory of the Scott-Russell mechanism and presents the gripper's mechanical structure and motion sequence. Section 4 provides a formulaic model for the grasping force at the Scott-Russell mechanism's end. Section 5 introduces the prototype and presents grasping experiments. Finally, Section 6 provides the conclusion.

II. RELATED WORK

A. Determination of Fingertip Trajectory

Through design, we can determine the direction of the fingertip's motion trajectory during environmental interaction. Figure 2 illustrates three classic fingertip grasping trajectories, demonstrating possible motion directions when interacting with planar surfaces.

If the fingertip moves along a right-diagonal trajectory, contact with the object causes both fingertips of the parallel gripper to converge toward the inner region of the grasping zone, reducing the effective grasping range. Subsequently, when the robotic arm approaches from above and presses the gripper downward against the supporting surface, the fingers bend under surface support, leading to spring deformation. At this point, the linear actuator can be engaged to grasp the object. However, as the fingertips passively converge during downward motion, improper gripper placement may cause grasping failure due to the diminished range. Even after a successful grasp, if the linear actuator fails to sustain force on the fingertips, the springs will restore the fingertips to their initial position, resulting in object drop.

If the fingertip follows a vertical trajectory, it avoids the issues associated with the right-diagonal motion but only adapts to flat, parallel surfaces. In environments with lateral protrusions or depressions, the vertical trajectory lacks lateral compliance, requiring active torque to overcome obstacles. This may cause excessive contact forces or motion jamming. Achieving compliance in this scenario still relies entirely on robotic arm control, as shown in Figure 2(b).

Regarding the grasping method using the left-diagonal trajectory, some literature dismisses it with claims like "the gripper cannot grasp an object with a width smaller than the opening distance between the fingertips.", simply adjusting the initial grasp position to be anterior to the finger base prevents the alleged issue that "the gripper cannot grasp objects narrower than the initial fingertip spread." Furthermore, due to the action of the springs, the finger mechanism itself provides a certain pressure on the object during grasping, enhancing grasp stability.

Due to the left-diagonal trajectory, the fingertip's motion direction incorporates both a vertical component and a horizontal component. When encountering irregular surfaces: The horizontal component can guide the fingertip to slide along the surface tangent or conform to the contour, reducing normal impact forces. The vertical component maintains essential contact pressure. The synergistic action of these components enables the finger to follow surface undulations more smoothly, significantly lowering jamming risks.

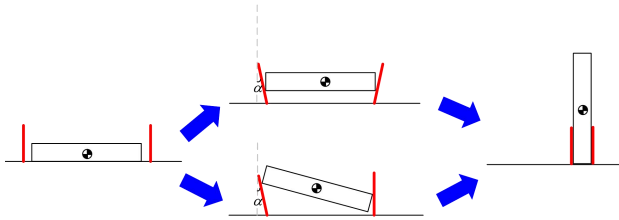


Figure 4. The two cases of scooping grasp: symmetric scooping and asymmetric scooping.

B. Implementation of Two Scooping Modes

The human hand employs two modes for scooping objects: symmetric scooping and asymmetric scooping. In the gripper, the scooping function can be achieved in two ways:

1. Passively: Leveraging angular changes within the parallelogram linkage as the robotic arm approaches the object, combined with the action of springs and stopper blocks.

2. Actively: Utilizing the second motor to drive the rotation of the base link of the parallelogram linkage, thereby actively rotating the fingertip.(Fig.8)

III. OPERATING PRINCIPLE OF THE SCOTT MECHANISM

To achieve the structure possessing the left-diagonal linear trajectory required for the aforementioned finger mechanism, we drew inspiration, identifying a straight-line mechanism—the Scott-Russell mechanism. This mechanism is a link-slider assembly, consisting of one slider and two links, as shown in Fig. 3. Due to its unique geometry, its end trajectory can generate a linear trajectory along AC as the angle between CB and BD varies.

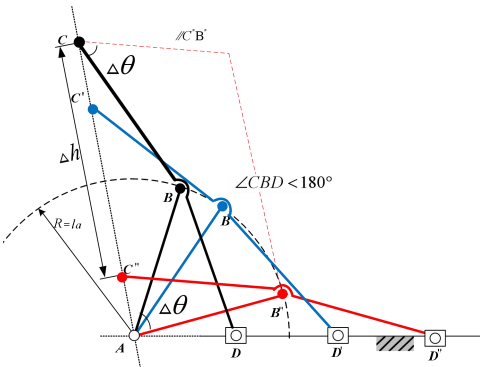


Figure 5. The Scott Russell mechanism can generate straight-line trajectories at various angles.

Its operating principle is shown in Figure 5. The key feature of this mechanism is that $AB=BC=BD$. The B on the circumference with A as the center and r (where r is a specific radius value) as the radius and the straight line AC is always the chord of the circle with B as the center and r (the radius here may have a specific relationship with the above-mentioned r, which needs to be determined according to the specific context) as the radius. It is precisely based on such geometric relationships that precise linear motion is achieved.

A. Linear Pinch Grip: Design of the Gamma-X Mechanism Based on the Scott Linkage and Parallelogram Mechanism

Figure 5 shows the relationship between Δh and $\Delta\theta$ when the Scott linkage is in vertical motion.

We define the linkage parameters as follows: l_{AB} , l_{CB} and l_{AD} represent the length of the first finger segment, the second finger segment and the distance between the origin and the slide rail respectively. l_{CBD} is the drive linkage, which enables the tip point C to move precisely along a straight line. The relationships among the parameters of these linkages can be obtained through formulas, so as to better set the initial state of the fingers and enable the fingers to better respond to external forces. The mechanical characteristics of the Scott mechanism itself are:

$$l_{BD} = l_{AB} = l_{BC} \quad (1)$$

In the initial state, l_{AD} satisfies the following relationship:

$$l_{AD} = 2l_{AB} \cos \angle BAD \quad (2)$$

The distance l_{AC} from the distal joint axis to the finger base satisfies:

$$l_{AC} = 2l_{AB} \sin \angle BAD \quad (3)$$

Set the length of the first finger segment as previously determined $l_{AB} = 100\text{mm}$, $\angle BAD = 70^\circ$, The corresponding values of $l_{AD} = 188\text{ mm}$ and $l_{AC} = 68.4\text{ mm}$, along with l_{AB} , l_{AD} , l_{AC} and angle $\angle BAD$, are stored in Table 1.

TABLE 1. Dimension Parameters of the Gamma-X finger

Predetermined parameters		Designed parameters	
l_{AB}	$\angle BAD$	l_{AC}	l_{AD}
100mm	70°	188mm	68.4mm

In addition, as shown in Figure 6, a spring k1 is installed at joint B to enable the finger to extend after bending, achieving

its compliance. A limit block Q1 is set at joint A, with $Q_1=20^\circ$, to ensure the stability of the finger's initial state.

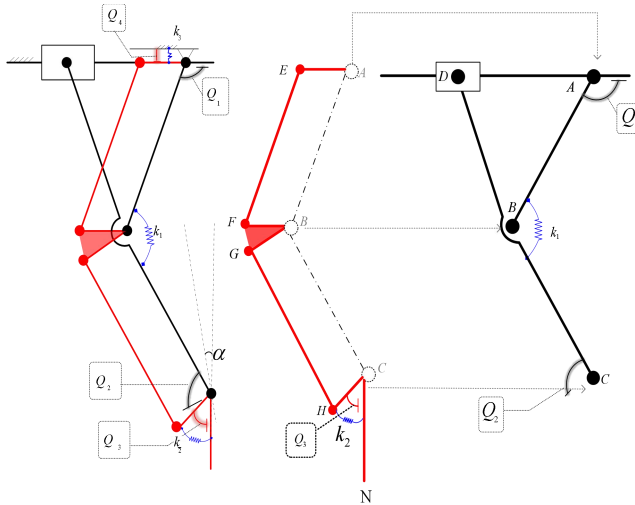


Figure 6. The principle of the Gamma-X finger.

B. Tip rotation: When the Gamma-X gripper meets the environment, it passively switches to the scooping mode.

As shown in Figure 6, the parallelogram mechanism and the Scott mechanism share joints A, B and C. This arrangement makes the overall structure of the finger more compact. The stability of the parallelogram when gripping flat objects allows a pair of Gamma-X mechanisms to grasp objects more stably.

The fingertip of this manipulator can achieve two scooping postures in coordination with the robotic arm. Scooping can guide objects that cannot be directly grasped by flat clamping into the range where the gripper can grasp them and then perform pinching or enveloping operations.

A limit block Q_2 is set on link CD and a limit block Q_3 is set on link CH, with the angle designed as $Q_3 = 52.5^\circ$ ($\angle FBG = 40^\circ$). It works with spring k_2 to provide vertical support for fingertip CN. Q_2 is the key to triggering the scooping posture and its function and the conversion process of the scooping posture are shown in Figure 7.

As shown in Figure 7, when the gripper is pushed downward and the height difference has not reached Δh_1 , Q_3 and k_2 can provide good support.

When the height displacement reaches Δh_1 , Q_2 meets the fingertip. Further downward pressure can cause Q_2 to push the fingertip to one side, forming an angle of attack, while overcoming the pressure of spring k_2 . We can refer to $0 \leq \Delta h_1$ as the flat clamping range.

When the height displacement reaches and joint D reaches the end of the guide rail, the scooping posture is completed. We can refer to $\Delta h_1 \leq h \leq \Delta h_2$ as the scooping range. The angle of Q_2 is set to 150° . The size of the angle of attack is related to the angle setting of Q_2 and the length l from the origin to the end of the track, satisfying:

$$\cos \theta = l / (2l_{oc}) \quad (4)$$

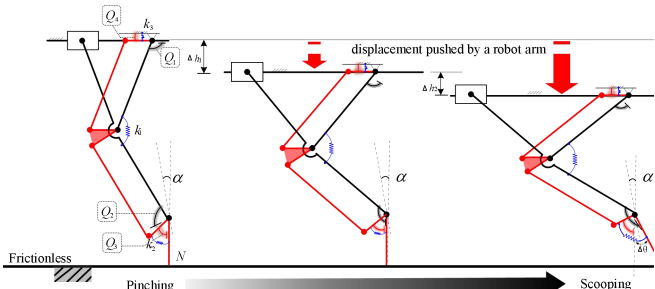


Figure 7. The fingertip posture transition from parallel pinching to scooping is achieved by the push of the limit block.

$$\theta = \arccos \theta \quad (5)$$

$$\Delta \theta = Q_2 - 90^\circ - \theta \quad (6)$$

Let the length l be 86.6 mm, at which point, when in the scooping posture, θ is exactly 30° . In this case, $\Delta \theta = 30^\circ$. All dimensions of the parallelogram and the limit blocks are listed in Table 2.

TABIE 2. The Parallelogram Mechanism and the Limit Block

Q_1	Q_2	Q_3	$\theta, \Delta \theta$	$\angle FBG$	AE, BF, CH, BG	CN
20°	150°	52.5°	30°	34.2°	60mm	30m m

C. Tip rotation: The Gamma-X gripper actively switches to the scooping mode via motor-driven actuation.

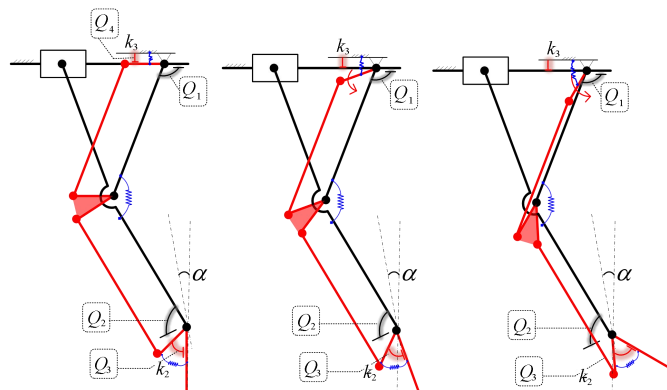


Figure 8. The entire process of motor-driven fingertip rotation.

In the active mode, Q_3 and the second motor actuation are key to triggering the scooping posture, its function, and the transition process. The core process involves the second motor driving the base link (AE) of the parallelogram linkage. Utilizing the coordinated action of Q_3 and k_2 , it provides thrust to induce fingertip rotation (as shown in Fig. 8). The final rotation angle of the fingertip can be programmatically controlled.

IV. THEORETICAL ANALYSIS

The core functionality of this device lies in achieving stable scooping actions, with its key mechanism relying on the coordinated motion between the limit block Q_2 and the distal fingertip during the scooping process. To ensure the reliability of the scooping motion, the following conditions must be satisfied: when the robotic arm is pressed downward into the target scooping range, Q_2 must continuously push the fingertip to form a stable angle of attack, with no relative displacement between them. This constraint is essentially a

static equilibrium problem, achieved through the rational configuration of the constrained force system acting on the fingertip, particularly the selection of the elastic coefficient k_2 for the spring element. To better validate the grasping performance of the gripper and investigate the influence of different inclined trajectory angles θ on the grasping force, we modeled the forces acting on the grasped object. The force model of the object satisfies the diagram in Fig. 9.

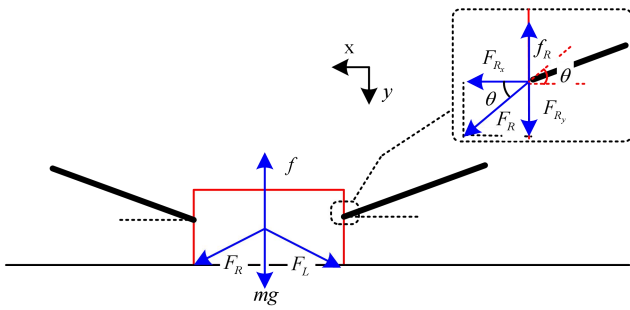


Figure 9. The relationship between grasping forces, frictions and angles.

From the force diagram, we observe:

$$\begin{cases} f_R = \mu F_{R_x} \\ f_L = \mu F_{L_x} \end{cases} \quad (7)$$

Therefore:

$$f = f_L + f_R = mg + F_{R_y} + F_{L_y} \quad (8)$$

Based on the relationship of the forces, we obtain:

$$F_{R_y} / F_{R_x} = \tan \theta \quad (9)$$

Substituting Equation (9) into Equation (8), we readily derive:

$$\mu F_{L_x} + \mu F_{R_x} = mg + F_{R_y} + F_{L_y} \quad (10)$$

Thus:

$$\mu(F_{L_x} + F_{R_x}) = mg + \tan \theta(F_{R_x} + F_{L_x}) \quad (11)$$

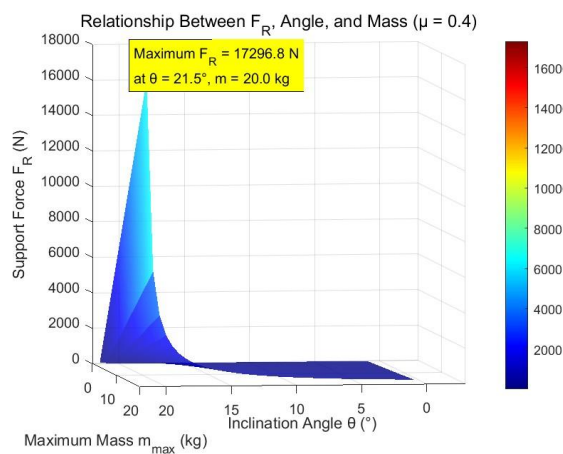


Figure 10. The relationship between F_R, θ, m .

We arrive at the mechanical relationship relating the grasping force (F), frictional coefficient (μ), and trajectory inclination angle (θ):

$$(F_{L_x} + F_{R_x})(\mu - \tan \theta) = mg \quad (12)$$

Let the maximum object mass that can be grasped be m_{\max} . Then we have:

$$2F_{Rx \max} = m_{\max}g / (\mu - \tan \theta) \quad (13)$$

This yields the final relationship between F , μ , and θ :

$$F_{R_{\max}} = m_{\max}g / (2(\mu - \tan \theta) \cos \theta) \quad (14)$$

Through formula analysis and visual plotting in MATLAB, we can see that a sudden change occurs when θ is around 10°.

V. GRASPING EXPERIMENT

To verify the design concept proposed in this paper, we designed a prototype and conducted grasping experiments with it to validate the three grasping methods of the Gamma-X mechanism. The entire prototype was printed using the “A1” printer Designed by Bambu Lab Company. PLA was prioritized in material selection because it strikes the best balance between cost - effectiveness and functional requirements.

A. Prototype Design

As shown in Figure 11. The design of the gripper prototype is carried out through 3D modeling in SolidWorks and the parts are made using the Bambu Lab A1 3D printer. By adapting to the flange interface, the prototype can be better matched with the robotic arm.

A 2-mm-deep groove is designed on the contact surface between the Gamma-X fingertip and the object and a 2-mm-thick textured silicone plate is bonded inside the groove to optimize the surface interaction. Compared with the bare PLA material, the textured silicone plate can provide greater friction, making the grasping more stable. Meanwhile, its elasticity allows it to better simulate the mechanical characteristics of human fingertips.

B. Spring Selection

Within the Gamma-X mechanism, the stiffness of a spring (i.e., the spring constant k) directly impacts its restoring force and the collaborative performance of morphological transformation. Through experimental verification, we have found that improper spring design can lead to three scenarios

When the elastic force of spring k_1 is too large, during the pressing process, the Gamma-X mechanism is not prone to vertical compliance, which can easily lead to rigid collisions and it is also difficult to achieve the adaptive functionality of the object

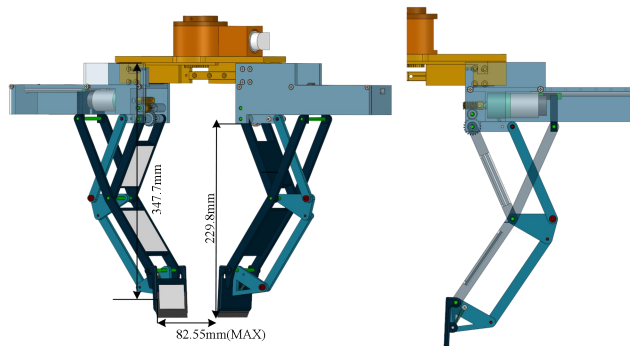


Figure 11. Overall view of the Gamma-X gripper.

When the elastic force of spring k_2 is too small, it is insufficient to provide the fingertip recovery force and thus cannot support the stability of the scooping grasp.

C. Environmental interaction capability

The prototype has good environmental interaction capability, and scooping can be passively achieved by pressing. Among them, asymmetric scooping requires adjusting the gripper angle.

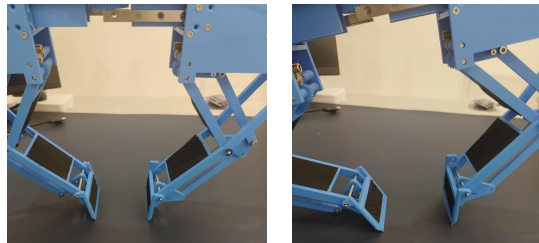


Figure 12. The passive realization of symmetric scooping and asymmetric scooping, respectively.

D. Second motor drive

The effect diagram of the second motor drive is shown in Figure 13.

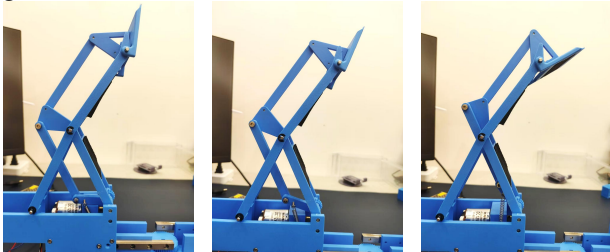


Figure 13. When the motor actively drives the distal phalanx, the rotational process of the distal phalanx.

Through the coordination among the limit block, spring, and motor, its function meets the expectations of our theoretical analysis.

E. Grasping Experiments

We aimed to verify the scooping capability of the second motor drive for objects and the stability and feasibility of grasping thin objects in the scooping state. To this end, we grasped thin paper sheets and a cylindrical object, and the grasping was successful.

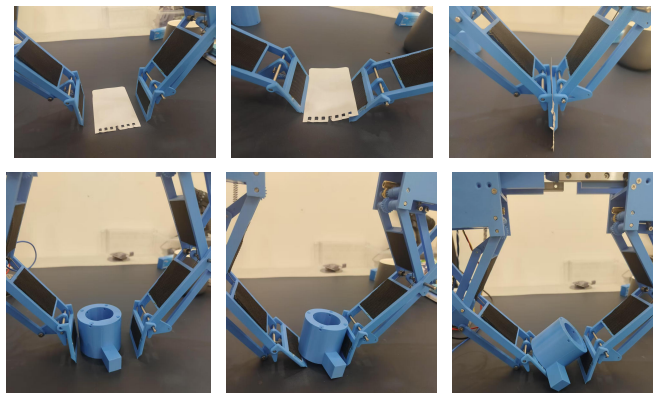


Figure 14. Grasping a piece of paper and adjusting the object's position within the fingers by scooping it.

VI. CONCLUSIONS

This paper proposes an underactuated adaptive robot gripper (Gamma-X gripper) based on the Scott linkage mechanism, which has achieved multi-modal grasping capabilities under environmental constraints through mechanical innovation. The research results show that: the design utilizes the linear motion characteristics of the Scott linkage, replacing the traditional multi-link mechanism with a refined 4-link structure, significantly reducing manufacturing costs while maintaining vertical compliance. Through the coupled design of spring limitation and parallelogram mechanism, the gripper can autonomously switch between four grasping modes: parallel grasping, symmetrical scooping, asymmetrical scooping and adaptive enveloping and has successfully completed stable grasping of cards, cylinders and irregular objects in experiments. This robot gripper has great potential to replace the widely used four-bar mechanism.

REFERENCES

- [1] Wei Jia et al. "Real-Time Interactive Capabilities of Dual-Arm Systems for Humanoid Robots in Unstructured Environments," *IEEE Int. Conf. on Automation Science and Engineering (CASE)*, 2024.
- [2] Y. Kageyama et al., "Learning Scooping Deformable Plastic Objects using Tactile Sensors," *Int. Conf. on Automation Science and Engineering (CASE)*, pp. 4020-4025, 2024
- [3] L. U. Odhner, R. R. Ma, and A. M. Dollar, "Open-loop precision grasping with underactuated hands inspired by a human manipulation strategy," *IEEE Trans. Autom. Sci. Eng.*, Jul. 2013
- [4] Q. Zhang, et al., "Prying grasp for picking thin object using thick fingertips," *IEEE Robotics and Automation Letters*, vol. 7, no. 4, pp. 11577-11584, Oct. 2022,
- [5] F. Lévesque, et al., "A model-based scooping grasp for the autonomous picking of unknown objects with a two-fingered gripper," *Robotics and Autonomous Systems*, 2018.
- [6] V. Babin, et al., "Stable and repeatable grasping of flat objects on hard surfaces using passive and epicyclic mechanisms," *Robotics and Computer Integrated Manufacturing*, vol. 55, pp. 1-10, 2019
- [7] H. Cha, et al., "High-speed scooping through dynamic manipulation: Model and practice," *IEEE Robotics and Automation Letters*, vol. 10, no. 2, pp. 1377-1384, Feb. 2025
- [8] K. H. Mak and J. Seo, "High-speed scooping manipulation using controlled compliance," *RSS Workshop on High-Speed Robotics*, 2022
- [9] H. Cha, I. Lee, and J. Seo, "High-speed scooping through dynamic manipulation: Model and practice," *IEEE Robotics and Automation Letters*, 2025
- [10] T. He, et al., "Scooping manipulation via motion control with a two-fingered gripper and its application to bin picking," *IEEE Robotics and Automation Letters*, Oct. 2021.
- [11] T. Ko, "A tendon-driven robot gripper with passively switchable underactuated surface and its physics simulation-based parameter optimization," *IEEE Robotics and Automation Letters*, 2020
- [12] N. Correll, et al., "Analysis and observations from the first Amazon Picking Challenge," *IEEE Trans. Autom. Sci. Eng.*, vol. Jan. 2018
- [13] Hajji-Ahmad, et al., "GRASP: Grocery Robot's Adhesion and Suction Picker," *IEEE Robotics and Automation Letters*, vol. 8, no. 10, pp. 6419-6426, Oct. 2023
- [14] Babin, V., & Gosselin, C. "Picking, grasping, or scooping small objects lying on flat surfaces: a design approach." *Int. J. Robotics Research*, 37(12), 1484-1499. 2018
- [15] Yoon D. and Kim K., "Fully Passive Robotic Finger for Human-Inspired Adaptive Grasping in Environmental Constraints," *IEEE/ASME Trans. on Mechatronics*, Vol. 27, No. 5, pp: 3841-3852. 2022.